Novel Form Birefringence Modeling for an Ultracompact Sensor in Porous Silicon Films Using Polarization Interferometry

Beom-hoan O, Chul-Hyun Choi, Soo-Beom Jo, Min-Woo Lee, Dong-Gue Park, Byeong-Gwon Kang, Sun-Hyung Kim, Rong Liu, Yang Yang Li, Michael J. Sailor, and Yeshaiahu Fainman

***Abstract*—The optical form birefringence in porous silicon films is measured by analyzing the transmitted interference intensity of a polarization interferometer. A novel form birefringence model called "boundary condition (BC) model" for porous materials is introduced and evaluated experimentally against samples of porous silicon films. The variation of optical indexes of refraction vs the porosity in silicon films agrees with the calculated values of n_o/n_e within 1% error using the BC model, in contrast to the ∼15% error using effective medium approximation model.**

***Index Terms*—Birefringence, boundary condition (BC) model, effective medium approximation (EMA), polarization interferometer, porous silicon (PSi), simulation.**

POROUS silicon (PSi) has attracted much attention and the techniques of fabrication and characterization of PSi have been established [1]. The optical birefringence in fabricated PSi films shows discrepancy between the calculations using existing models and the experimentally measured ones in birefringence [2]–[4] as well as of reflectivity [5]. In this manuscript, we introduce a novel "boundary condition (BC) model" and evaluate the performance of this model for the characterization of optical birefringence in PSi films. The BC model not only accurately predicts optical indexes n_e and n_o from the structural information of such an artificial nanostructured inhomogeneous materials, but also traces the variation of optical birefringence vs the porosity $f_{\rm air}$ (= volume of air pores/total volume) of the materials, making it useful for various device engineering.

Due to the cylindrical symmetry of the PSi film with micropores distributed uniformly on the surface [4], the resulting artificial form birefringence can be described similar to that of a positive uniaxial anisotropic crystal leading to the rotationally symmetric index ellipsoid with the eigenvalues (n_o, n_o, n_e) in the principal coordinate system (see Fig. 1). The basic analytic equations for effective permittivities, which is analogous to the serial/parallel capacitor problem in a circuit, can be obtained easily by balancing effective energy of a microscopic volume including just one air pore for a simple BC of electric field. Our model, for the sake of simple derivation of analytic index equations, simplifies the shape of air pores by assuming square pillars that will have only one or two types of walls leading to BCs parallel and perpendicular to the electric field of the optical wave. Then, $\varepsilon_{\rm eff} = \varepsilon_1(A_1/A) + \varepsilon_2(A_2/A)$ for the parallel BC case, and $1/\varepsilon_{\rm eff} = (L_1/L)/\varepsilon_1 + (L_2/L)/\varepsilon_2$ for perpendicular BC case. $A(= A_1 + A_2)$ is for area, and $L(= L_1 + L_2)$ for the length [6]. The value of extraordinary index of refraction n_e for PSi can be determined from the parallel BC approximation as the electric field is parallel to z-axis, and thus parallel to all boundary walls of air pores (see Fig. 1). In contrast, the calculation of ordinary index n_o requires both parallel and perpendicular types of walls, as the electric field is on the surface of the film. The analytic equations refined for form-birefringent dielectrics are given as follows:

$$n_o = \sqrt{(1 - K\cdot\beta)\varepsilon_{\rm Si} + K\cdot\beta\frac{\varepsilon_{\rm Si}\cdot\varepsilon_{\rm Air}}{\beta\cdot\varepsilon_{\rm Si} + (1-\beta)\varepsilon_{\rm Air}}} \quad (1)$$

$$n_e = \sqrt{\beta^2\cdot\varepsilon_{\rm Air} + (1-\beta^2)\cdot\varepsilon_{\rm Si}} \quad (2)$$

where $\beta = \sqrt{f_{\rm air}}$, $f_{\rm air}$ is the porosity, K is an arbitrary correction factor, and $\varepsilon_{\rm air}$ and $\varepsilon_{\rm Si}$ are the permittivities of air and silicon, respectively. The correction factor K is introduced to account for the distortion of electric flux without significant change in n_o, and K will be set to $K_{\rm simpleBC} \equiv 1$ for a "simple BC model," and $K = K_{\rm BC} \equiv \beta^{1/8} + (1-\beta^{1/8})\cdot 2\varepsilon_{\rm Air}/(\varepsilon_{\rm Si}\cdot[\varepsilon_{\rm Air} + \varepsilon_{\rm Si}])$ for a "BC model." Notice that the factor $K_{\rm BC}$ approaches to $2\varepsilon_{\rm Air}/(\varepsilon_{\rm Si}\cdot[\varepsilon_{\rm Air} + \varepsilon_{\rm Si}])$ for extremely low porosity as $f_{\rm air}^{1/16} \sim 0$, otherwise $K_{\rm BC}$ is also nearly 1 because

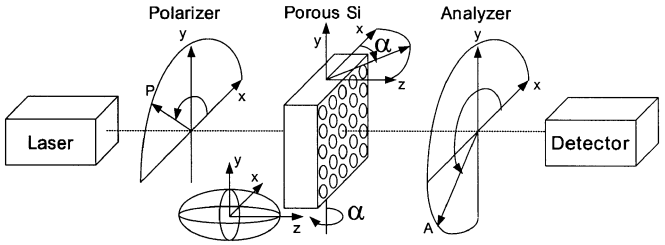

Fig. 1. Schematic diagram of experimental setup and the index ellipsoid of a Psi film.

Manuscript received June 17, 2003; revised September 16, 2003. This work was supported by the National Science Foundation, by the Office of Naval Research, by DARPA/SPAWAR, and by the Korea Science and Engineering Foundation under Grant R11-2003-022.

B. O, C.-H. Choi, S.-B. Jo, and M.-W. Lee are with the School of Information and Communications, INHA University, Incheon 402-751, Korea (e-mail: obh@inha.ac.kr).

D.-G. Park, B.-G. Kang, and S.-H. Kim are with the Information and Technology Engineering Department, Soon Chun Hyang University, Choong Chung Nam Do, Korea (e-mail: dgpark@sch.ac.kr).

R. Liu and Y. Fainman are with the Department of Electrical and Computer Engineering, University of California at San Diego, La Jolla, 92093 CA USA.

Y. Y. Li and M. J. Sailor are with the Department of Chemistry and Biochemistry, University of California at San Diego, La Jolla, 92093 CA USA.

Digital Object Identifier 10.1109/LPT.2003.821096

$f_{\rm air}^{1/16} \sim 1$. Thus, expanding (1) as a polynomial of β leads to $n_o = \sqrt{\varepsilon_{\rm Si} - f_{\rm air} \cdot 2 \cdot (\varepsilon_{\rm Si} - \varepsilon_{\rm Air})/(\varepsilon_{\rm Si} + \varepsilon_{\rm Air})}$ for a two–dimensional (2-D) dielectric model with sparse cylindrical air impurity. Note that a typical three–dimensional (3-D) dielectric model for spherical air impurity gives $n_o = \sqrt{\varepsilon_{\rm Si} - f_{\rm air} \cdot 3 \cdot (\varepsilon_{\rm Si} - \varepsilon_{\rm Air})/(2 \cdot \varepsilon_{\rm Si} + \varepsilon_{\rm Air})}$ [6], which is valid only when impurities are sparse ($f_{\rm air} \sim 0$) and so far apart enough not as to affect one another. In the following we evaluate the validity of the equations for n_e and n_o [i.e., (1) and (2)] in the case of dense inhomogeneity range in PSi films with various porosity.

PSi films are fabricated from highly doped p-type $\langle 100 \rangle$ silicon wafer by anodic etching in aqueous HF (49 wt%) solution with ethanol in the volume ratio of 3:1 at room temperature [7]. An atomic-force microscope was used to determine the average pore size of less than 20 nm in width, whereas the porosity was controlled to vary for different samples from ~70% to ~85%, estimated using gravimetric method. As explained in introduction, this porous film has optic axis collinear with the direction of the pores. Consequently, the effective dielectric constant for optical field polarized in the plane of incidence (i.e., TM or extraordinary polarization) will depend strongly on the angle of incidence [7]. A schematic diagram of our experimental setup for characterization is shown in Fig. 1.

The wavelength of an external-cavity tunable laser source of 1.52 μm is chosen below the band edge of silicon to minimize optical absorption loss. The porous silicon sample is mounted on a precision rotation stage, allowing precise control of the surface normal orientation. The propagation direction of the optical beam is set first at $\alpha = 0$ to be collinear with the z axis (i.e., the pores) of the PSi film. The polarizer and analyzer are aligned perpendicular with respect to each other and at 45° with the x axis in the x–y plane. When the angle α in the z–x plane is increased from zero, we find the transmitted intensity at the output of the analyzer

$$I(\alpha) = \frac{1}{2}\left[a^2 + b^2 - 2ab\cos\left(\Delta\phi(\alpha)\right)\right] \tag{3}$$

$$\Delta\phi(\alpha) = \frac{2\pi}{\lambda}\left[n_e(\alpha)L_e(\alpha) - n_o(\alpha)L_o(\alpha)\right] \tag{4}$$

where a and b are the amplitudes of transmitted electric fields for ordinary (perpendicular to the plane of incidence, TE) and extraordinary (in the plane of incidence, TM) polarizations, respectively, $\Delta\phi(\alpha)$ is the effective phase difference for ordinary and extraordinary polarized components, and λ, $n_{e(o)}(\alpha)$, and $L_{e(o)}(\alpha)$ are the laser wavelength in vacuum, angle dependent effective refractive indexes, and the geometric path lengths in a film for extraordinary (ordinary) component for a given rotation angle α, respectively. Note that $n_o(\alpha) = n_o$ (ordinary index) for all α and $n_e(\alpha)$ is $1/\sqrt{\cos^2\alpha/n_o^2 + \sin^2\alpha/n_e^2}$ in this setup, where n_e is an extraordinary index of the index ellipsoid. The polarization interference signals are obtained by measuring the transmitted optical intensity for each PSi film sample [7]. This intensity variations are simulated by a homemade code for this birefringence measurement. The measured and simulated polarization interference signals versus the angle of incidence are shown in Fig. 2.

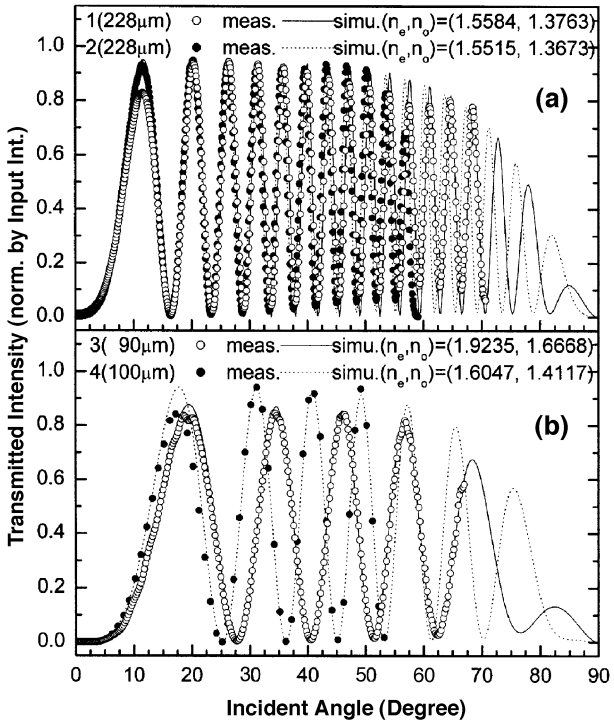

Fig. 2. Comparison of the polarization interference signals through a porous silicon film as a function of incident angle (a) for two films of same thickness of 228 μm with slightly different porosity of 0.875 and 0.873 and (b) for two films of similar thicknesses of 90 and 100 μm, but with quite different porosity of 0.86 and 0.76.

Note that the chirp-like behavior of the transmitted intensity from the effective phase difference, $\Delta\phi(\alpha)$, helps the curve fit process to determine unique optical index values n_e and n_o [7], which are varied independently to find the best intensity curve fit. The index pair values (n_e, n_o) of the best fit and the corresponding error ranges for all cases are summarized for comparison in Table I. The intensity curves simulated with the index pairs at upper/lower values in Table I show large deviation of out of tolerance from the measured ones. Note that the error range decreases as the film thickness increases due to the increase of phase lag, leading to more phase variation data for accurate curve fit.

We also investigate the dependence of refractive indexes on the film porosity for various models [see Fig. 3(a)]. The refractive indexes from using the BC model is compared with that of the Bruggeman's effective medium index approximation (EMA) in Fig. 3(b). It reveals apparent agreement of the measured results with the BC model.

The inset figures in Fig. 3(a) represent the simplified cross sections for microscopic BCs with the direction of electric field denoted by an arrow. The first figure from the left is for $n_{o,\rm layered}$ of layered structure, the second one for $n_{o,\rm Sep.Si}$ of isolated Si column structure, the third for $n_{o,\rm BC}$ or $n_{o,\rm simpleBC}$ of isolated air pore structure of PSi films, and the last one corresponds to n_e of layered or pillar structure of PSi films with surface parallel to electric field. Note that $n_{o,\rm BC}$ is similar to that of $n_{o,\rm simpleBC}$ for all $f_{\rm air}$ (just slightly larger than). It should also be noticed that the curve for $n_{o,\rm Sep.Si}$ is much lower than that for $n_{o,\rm simpleBC}$, although the only difference in structure is the connectivity of

TABLE I
COMPARISONS OF OPTICAL INDEXES, ERROR RANGE, AND POROSITY VALUES FOR VARIOUS PSi FILM SAMPLES

PSi film	Porosity (Gravimet.)	Porosity (BCmodel)	$(n_e, n_o)_{lower}$	$(n_e, n_o)_{best}$	$(n_e, n_o)_{upper}$	$(\pm\Box n_e, \pm\Box n_o)$
72 (μm)	0.82	0.85	(1.5330, 1.3728)	(1.6394, 1.4533)	(1.7395, 1.5283)	(±0.10, ±0.08)
90 (μm)	0.71	0.76	(1.8641, 1.6248)	(1.9235, 1.6668)	(1.9812, 1.7079)	(±0.06, ±0.04)
100 (μm)	0.82	0.86	(1.5330, 1.3590)	(1.6047, 1.4117)	(1.6733, 1.4618)	(±0.05, ±0.05)
198 (μm)	0.82	0.83	(1.6733, 1.4635)	(1.7066, 1.4877)	(1.7393, 1.5117)	(±0.033, ±0.024)
228 (μm)	0.82	0.873	(1.5330, 1.3582)	(1.5584, 1.3763)	(1.5871, 1.3971)	(±0.026, ±0.019)
228 (μm)	0.82	0.875	(1.5330, 1.3541)	(1.5515, 1.3673)	(1.5692, 1.3803)	(±0.018, ±0.013)

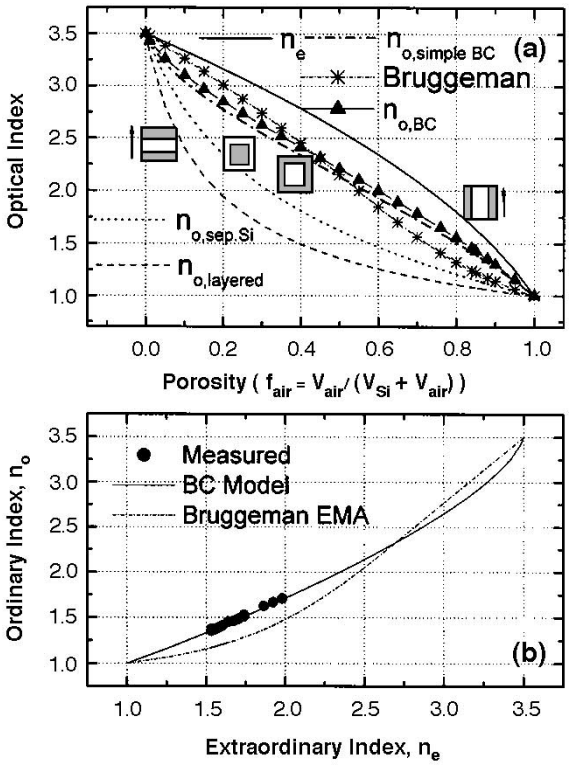

Fig. 3. Comparison of (a) index curves from various models as a function of porosity and (b) index pair coordinates of (n_e, n_o) in the index plane. Four different diagrams in (a) denote simplified microscopic geometric arrangements of pores. The arrow represents the direction of the electric field.

Si. The value for $n_{o,\mathrm{layered}}$ comes from an unrealistic BC that all boundaries are always perpendicular to the field, only obtainable for layered structure. The resultant value of $n_{o,\mathrm{layered}}$ curve is the lowest for any f_{air} among all refractive index curves. Furthermore, $n_{o,\mathrm{Sep.Si}}$ is larger than $n_{o,\mathrm{layered}}$ due to the contribution of the increased effective Si area at the center region for the same f_{air}, as shown in the inset figure of simplified microscopic cross section. The value n_o calculated from EMA, which satisfies $n_o = \sqrt{\varepsilon_{av}}$ and $0 = \sum_i f_i\{(\varepsilon_i - \varepsilon_{av})/(\varepsilon_i + 2\varepsilon_{av})\}$, deviates much from the measured values, and it is larger than $n_{o,\mathrm{BC}}$ for low porosity $(f_{\mathrm{air}} <\sim 0.4)$ and smaller than $n_{o,\mathrm{BC}}$ for high porosity $(f_{\mathrm{air}} >\sim 0.5)$. The correlation between optical indexes n_e and n_o for various porosities can be viewed more easily in Fig. 3(b). It is apparent that the BC model agrees with the measured index values, while the curve from EMA somewhat deviates from the measured values. The introduced BC model with simple analytic expression provides a convenient and accurate prediction for the optical indexes for form birefringence in PSi film.

In summary, we proposed a novel optical index model, called "BC model," for the optical form birefringence of PSi films, and evaluated it experimentally by comparing the predicted indexes to the measured ones. The optical indexes of PSi films was characterized accurately using optical measurements based on the data from polarization interferometer. The optical indexes of PSi films are predicted much more accurately by the BC model than any other pre-existing models, to the best of our knowledge.

REFERENCES

[1] A. G. Cullis, L. T. Canham, and P. D. J. Calcott, "The structural luminescence properties of porous silicon," *J. Appl. Phys.*, vol. 82, no. 3, pp. 909–965, 1997.

[2] J. Diener, N. Kunzner, D. Kovalev, E. Gross, V. Yu. Timoshenko, G. Polisski, and F. Koch, "Dichroic Bragg reflectors based on birefringent porous silicon," *Appl. Phys. Lett.*, vol. 78, pp. 3887–3889, 2001.

[3] E. Gross, D. Kovalev, N. Kunzner, V. Yu. Timoshenko, J. Diener, and F. Koch, "Highly sensitive recognition element based on birefringent porous silicon layers," *J. Appl. Phys.*, vol. 90, pp. 3529–3532, 2001.

[4] S. Zangooie, R. Jansson, and H. Arwin, "Investigation of optical anisotropy of refractive-index-profiled porous silicon employing generalized ellipsometry," *J. Mater. Res.*, vol. 14, pp. 4167–4175, 1999.

[5] P. A. Snow, E. K. Squire, and P. St. J. Russell, "Vapor sensing using the optical properties of porous silicon Bragg mirrors," *J. Appl. Phys.*, vol. 86, pp. 1781–1784, 1999.

[6] J. D. Jackson, *Classical Electrodynamics*, 2nd ed. New York: Wiley, 1975, sec. 4.4–5, pp. 147–155.

[7] B. O, R. Liu, Y. Y. Li, M. J. Sailor, and Y. Fainman, "Vapor sensor realized in an ultra-compact polarization interferometer built of a free-standing porous silicon form birefringent film," *Photon. Technol. Lett.*, vol. 15, pp. 834–836, 2003.